IEEE Access
Multidisciplinary | Rapid Review | Open Access Journal

Received July 3, 2019, accepted July 10, 2019, date of publication July 15, 2019, date of current version August 1, 2019.

Digital Object Identifier 10.1109/ACCESS.2019.2928683

Low-Cost 3D-Printed Coupling-Fed Frequency Agile Fluidic Monopole Antenna System

CRISTINA BORDA-FORTUNY, (Member, IEEE), LINYU CAI, (Student Member, IEEE), KIN FAI TONG, (Senior Member, IEEE), AND KAI-KIT WONG, (Fellow, IEEE)
Department of Electronic and Electrical Engineering, University College London, London WC1E 7JE, U.K.

Corresponding author: Kin Fai Tong (k.tong@ucl.ac.uk)

This work was supported in part by the Engineering and Physical Sciences Research Council (EPSRC), U.K., under Grant EP/M016005/1. The work of C. Borda-Fortuny was supported by the University College London Security Science Doctoral Training Centre (UCL SECReT DTC), EPSRC, under Grant EP/G037264/1.

ABSTRACT A low-cost 3D-printed frequency agile fluidic monopole antenna system is demonstrated to respond to the increasing demand for reconfigurable antennas, which can operate in a dynamic environment, in this paper. Antennas that can be reconfigured for different operating frequencies, polarizations, or radiation patterns are attracting attention. Traditional reconfigurable antennas using a metallic radiating element with electronic switches are limited by their pre-defined physical geometries. As conductive fluid, either liquid metal or ionized fluid has no defined shape, so it is possible to create the desired shape of a fluidic antenna to support different wireless environments. The fabrication of the leakage-free containers for fluidic antennas needs special consideration, and stereo-lithography-based 3D-printing technology is a possible option to support the fabrication. Moreover, researchers will have higher design freedom and accuracy to create new container shapes for fluidic antennas. The fluidic monopole antenna proposed is coupling-fed by a ring geometry for separating the electrical and mechanical structures; such an approach enables individual optimization and minimizes mutual disturbances in the system. A parametric study of the proposed coupling-feed geometry and the experimental verification of the antenna prototypes have been performed. Reasonable frequency agility from 3.2 to 5 GHz has been demonstrated, and the peak efficiency is about 80%. A maximum gain of 3.8 dBi is obtained. The radiation patterns of the antenna are stable across the operating bandwidth. The proposed antenna could be useful for the applications in the recent 5G mid-bands operations.

INDEX TERMS 3D-printing, antennas, closed loop system, fluidic antennas, fluid control methods, monopole antennas, multifrequency antennas, omnidirectional antennas, reconfigurable antennas.

I. INTRODUCTION

Signal quality plays an important role in wireless communication systems, particularly the latest Internet of things (IoT) and the 5th generation mobile network (5G) technologies. An antenna is the first and also the last component in a wireless communication system; its performance would determine the data speed and reliability of the system. The radiating elements of the conventional antennas are usually made of metals. These materials usually have high conductivity and provide strong mechanical stability. However, the shapes of these metallic radiating elements are pre-defined in the design stage, so the agility the antennas is limited. In particular, modern wireless communications requires the antennas to be multi-functional and adaptive to the dynamic environment in both far and near proximity. Many attempts have been reported to improve the reconfigurability of metallic antennas in the areas of operating frequency [1]–[3], bandwidth [4], [5] polarization [6], [7], and radiation pattern [8], [9], this is usually achieved by using electronic devices, such as PIN diodes or Micro-Electro-Mechanical System (MEMS) switches.

Low-cost radio frequency (RF) switches are usually lossy and the metal strip biasing circuits could be difficult to be embedded with the antennas [10]. These issues may affect the antenna performance significantly [11]. On the other hand, high performance RF switches, which can operate in the microwave or millimeter-wave frequency range for modern wireless systems, could be expensive [12]. Fluid has no defined shape; theoretically it is possible to create

The associate editor coordinating the review of this manuscript and approving it for publication was Abhishek Kandwal.

the desirable shape of an antenna for different diversities. Recently various highly conductive liquid metals, such as Galinstan, Eutectic Gallium-Indium (EGaIn) ($\sigma = 3.4$–3.46×10^6 Sm^{-1}) or mercury ($\sigma = 1.0 \times 10^6$ Sm^{-1}), based fluidic antennas had been reported [13]–[19]. In [13], as the antenna was not properly matched, total efficiency of about 45% was obtained, while the maximum measured gain of the dual-band slot antenna in [14] was 3.25 dBi. An annular slot antenna with surface integrated fluidic channels was presented in [15], the frequency tuning was achieved by using different fluids, the gain fluctuation incurred in changing the fluid may not be desirable for practical applications. In [16], the fluid was only used for disturbing the E-field in the metallic microstrip monopole antenna, this design presented difficulties for complete drainage of the distilled water from the fluidic channels to change the operating frequency of the antenna. Additionally, the proposed design does not generate a significant frequency tuning in the impedance bandwidth of the antenna. A maximum frequency shift of 25% is observed when loaded with water. Other designs proposed to use the fluid as the radiating structures of the antennas. A Yagi-Uda formation using liquid metal filled monopoles was presented in [17]. Galinstan was used to reconfigure a 5-element Yagi-Uda using 6 fluidic monopoles. By injecting the appropriate amount of fluid, the antenna could be tuned in frequency and gain, and its radiation pattern could also be steered. However, the design was actuated manually using syringes, the repeatability of antenna performance cannot be guaranteed. Furthermore, it was not presented as a continuously tuning system. The two prototypes presented operated at 2.4 GHz and 3.87 GHz. Reference [18] presented a tunable mercury monopole, the measured gain obtained was between 0.5 dBi to 2.3 dBi with a maximum simulated efficiency of 54%. This design had a multiband operation in the lower band configuration which the frequency tuning was achieved by using two micro-pumps. These liquid metal designs achieved comparable performances with the ionized solution counterparts. However, as mercury is toxic and may raise safety concerns, while Galinstan and EGaIn are highly destructive to many other metals [22]–[24], such as aluminum and copper, by dissolving them; these issues set a barrier to widely use such liquid metals in general wireless systems.

On the other hand, ionized solutions, such as sodium chloride (NaCl) and potassium chloride (KCl) solution, and distilled water are easily accessible. Most importantly they are eco-friendly, so are the good alternatives for low-cost systems [20]–[22]. The fluid can be pumped into or out from a fluid container, such as a tube, to achieve the desirable dimensions for the particular operating frequency band.

In term of the tuning mechanism, the fluid in [16], [17] was manually controlled using syringes. Other designs used micro-pumps to inject fluid into the system and makes the tuning more automated [18]–[21]. To the authors' best knowledge, an automatic control for the frequency tuning with a closed-loop system is rare.

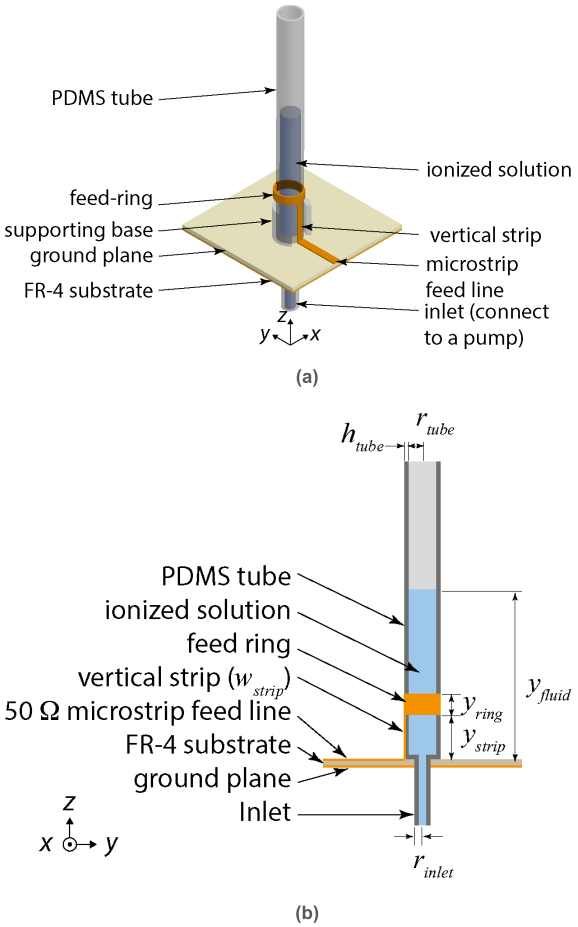

FIGURE 1. Geometry of the coupling-fed 3D printed fluidic monopole antenna, $r_{tube} = 2$ mm, $h_{tube} = 1$ mm, $r_{inlet} = 1.5$ mm, $w_{strip} = 1$ mm: (a) isometric view, (b) cross-sectional view.

In this paper, we propose a new design of fluidic antenna system to overcome the drawbacks of the traditional fluidic monopole antennas. The newly proposed coupling feed-ring geometry has the advantage that it does not directly contact with the ionized fluid, therefore the mechanical and electrical structures are separated, it gives the researchers more flexibility in creating new shapes for fluidic antennas and more importantly water leakage can be avoided. In addition, the optimization of the mechanical and electrical structures can be performed independently. High precision stereolithography (SLA) 3D-printing technology [26] is used for fabricating the leakage proof container. Finally, the closed-loop system which can automatically adjust the operating frequency in respond to the change of the communication channel condition is novel. CST microwave studio 2016 [27] was used in the simulation of the antenna performance.

II. ANTENNA GEOMETRY

The isometric and cross-sectional views of the coupling-fed fluidic monopole antenna are shown in Fig. 1. The antenna consists of four main parts: 1) a piece of 30 mm × 30 mm × 0.1 mm (L × W × h) FR- 4 substrate ($\varepsilon_r = 4.3$, $\tan\delta = 0.008$ @ 3 GHz) with a ground plane on the bottom side,

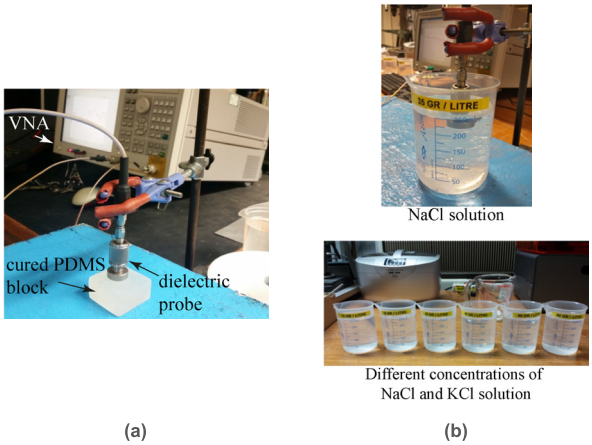

FIGURE 2. Equipment setup for measuring the dielectric properties of: (a) the container material (b) the ionized solutions.

TABLE 1. Concentration of the solutions.

Concentration (mol/liter)	NaCl (gram/liter)	KCl (gram/liter)
0.1	5.85	7.46
0.5	29.22	37.28
1	58.44	74.56
2	116.88	149.10

Weight of the NaCl and KCl salts for different concentrations of the solutions used in the antenna design.

2) a 3D-printed circular Polydimethylsiloxane (PDMS) tube for containing the ionized fluid, 3) a coupling feed geometry which consists of a 50 Ω microstrip feed line, a vertical strip, $y_{strip} = 4.5$ mm and a ring wrapped around circular tube, $y_{ring} = 1$ mm, and 4) A peristaltic pump, its digital control board and a Raspberry® Pi 2 [29]. The container tube for the ionized fluid is built using the standard clear resin with a Form 1+ Formlabs 3D printer. The resin is made with a mixture of methacrylic acid esters and photo-initiators that have dielectric property close to acrylic plastic. Experiments shown in Fig. 2 were set up to measure the actual dielectric parameters of the cured clear resin and the ionized solutions. An Agilent 85070E Dielectric Probe Kit was used to evaluate the dielectric constants and loss tangents of the PDMS tube and the two types of ionized solutions investigated in the paper. NaCl and KCl solutions of different concentrations from 0.1 mol/liter, 0.5 mol/liter, 1 mol/liter to 2 mol/liter were measured in the frequency range from 0.5 GHz to 8.5 GHz. The weight of the NaCl and KCl salts are tabulated in Table 1. The measured dielectric constants and loss tangents were fed back to the CST models for EM co-simulation to provide more accurate calculations for choosing the better ionized solution.

Weight of the NaCl and KCl salts for different concentrations of the solutions used in the antenna design.

III. ANTENNA OPERATION

The vertical cut of the simulated H-field of the proposed fluidic antenna is presented in Fig. 3. On the left-hand side, there is the microstrip feeding line. The radiation pattern agrees to

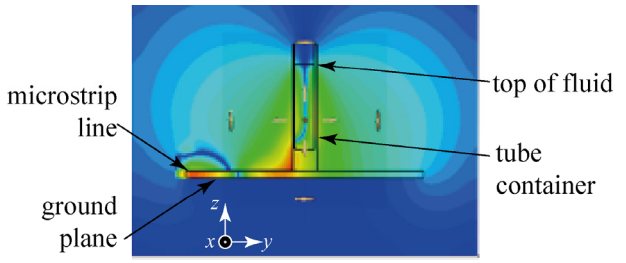

FIGURE 3. Simulated H-field of the AUT at 3.5 GHz.

that of a conventional monopole antenna. Moreover, it can be observed that the fluidic antenna operates like a monopole antenna with its quarter wavelength approximately equals to the height of the fluid (y_{fluid}). Also, as shown in Fig. 3, the source of the radiation comes through from the coupling feed-ring to the ionized solution.

A microstrip line is connected to a coupling feed-ring delivering the signal to the antenna. The top of the feeding-ring is 5 mm above the microstrip line surface. The feeding ring design allows the container to be completely watertight, as it does not require a direct contact with the ionized fluid in the tube. Also, the coupling feed provides a mechanism for wideband frequency tuning.

IV. FLUIDIC ANTENNA SYSTEM

Fig. 4a shows the fluidic antenna system, it consists of a fluidic monopole antenna, a R&S® FSH8 vector network analyzers (VNA) [29], a Raspberry Pi (RPi), a pump controller, a peristaltic pump, a plastic beaker with ionized solution serving as a reservoir, a silicone pipe connecting the antenna to the pump, a RF coaxial cables connecting the VNA to the antenna feed port, a USB cable connecting the VNA and the RPi. These components assemble the closed-loop system.

To monitor and control the whole system, a user interface was developed. Fig. 4b presents the workflow of the system. Once the operating frequency is determined according to the wireless channel condition, the pre-defined height of the ionized solution, which based on the previous experimental results, stored in the SD card of RPi will be set as the initial height of the fluidic antenna. The RPi will instruct the pump controller to pump in the ionized solution from the reservoir into the 3D-printed tube. At the same time, the S_{11} value of the fluidic antenna will be also monitored by the VNA and the results are feedback to the RPi for controlling the peristaltic pump operation. The pump is driven by a PWM signal using the micro-step method, which provides the high precision of flow rate and smooth rotation. A computer program is written for retrieving the S_{11} values from VNA, analyzing and comparing the real time data, then sending the corresponding commands to the VNAs and pumps. Based on the measured S_{11}, the RPi will decide whether to pump in or out the ionized solution to achieved the desirable operating frequency. A Satimo StarLab was used to measure the efficiency of the antennas in the operating frequency range.

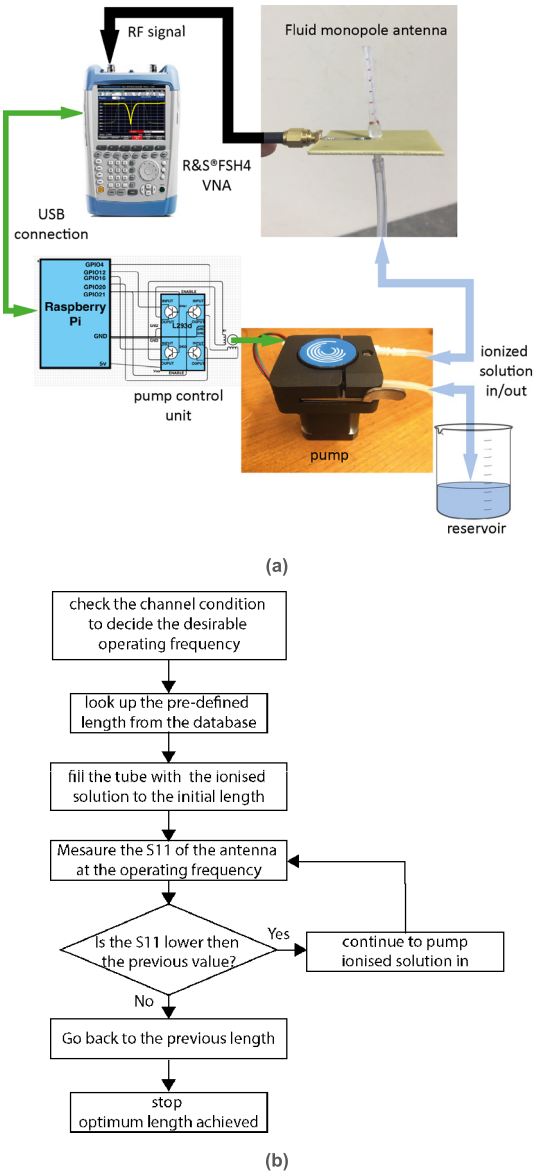

FIGURE 4. The fluidic antenna system components and how they are connected: (a) Diagram of the fluidic antenna system (b) Working flow diagram of the system.

V. PARAMETRIC STUDY OF THE COUPLING FEED GEOMETRY

As shown in Fig. 1a, the proposed coupling feed geometry consists of a 50 Ω microstrip line, a vertical strip and the feed-ring. The parametric studies of the height of the vertical strip (y_{strip}) and the width of the feed-ring (y_{ring}) have been performed to investigate the S_{11} of the antenna and provide the design guidelines of the proposed coupling feed geometry. In the parametric studies, the height of fluid length (y_{fluid}) is kept at 15 mm and the same PDMS tube model is used. The initial model is based on the optimum model described in Section II.

The S_{11} of the proposed antenna at different vertical strip heights (y_{strip}) is shown in Fig. 5. It can be observed that the minimum height should be higher than 3 mm for the proper

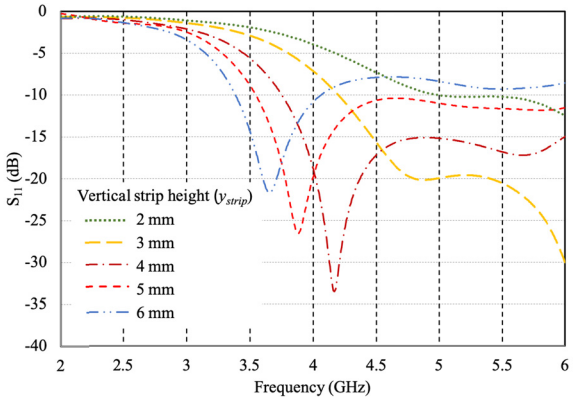

FIGURE 5. S11 of the proposed antenna at different vertical strip heights for $y_{ring} = 1$ mm and $y_{fluid} = 15.0$ mm.

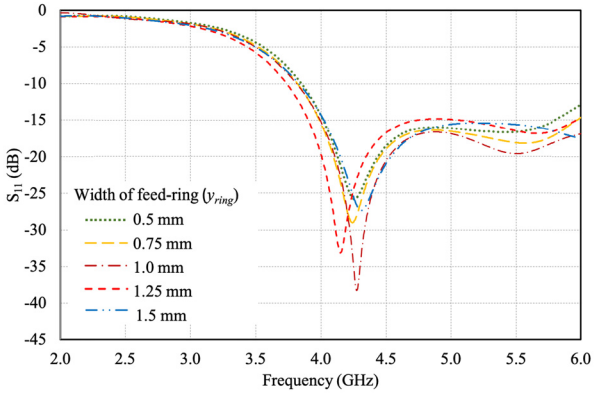

FIGURE 6. S11 of the proposed antenna at different widths of feed-ring for $y_{strip} = 3.5$ mm and $y_{fluid} = 15.0$ mm.

monopole operation of the antenna. When the height further increases beyond 3 mm, the operating frequency decreases. This feature can be utilized for deciding the center frequency of the frequency tuning range. For example, if an antenna operating at lower frequency band is required, a higher vertical height should be selected.

The effect caused by width of the feed-ring (y_{ring}) has also been investigated. The models of five different feed-ring widths in the range from 0.5 mm to 1.5 mm have been simulated. It can be observed from Fig. 6 that the width of the feed-ring can be used for fine tuning the impedance matching. When the width deviates from the optimum value, i.e. 1 mm in this case, the impedance matching is worse.

VI. RESULTS

Fig. 7 shows the measured S_{11}, in dB, from 2 to 6 GHz at different operating frequency bands of the optimized model. The simulated result for fluid height (y_{fluid}) equals 15 mm is also plotted in the figure for comparison. After considering the balance between conductivity and dielectric loss, ionized solution of 0.1 mol/liter NaCl was selected in the simulation and measurement. As expected the fluidic antenna system presents different operating frequency bands depending on the height of the ionized fluid that is pumped into

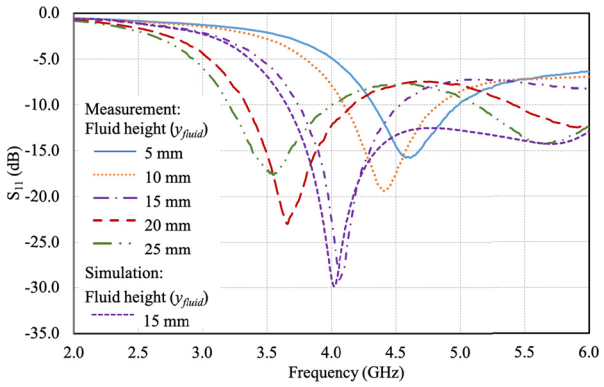

FIGURE 7. Measured S_{11} parameter (dB) over frequency of the AUT at different fluid heights.

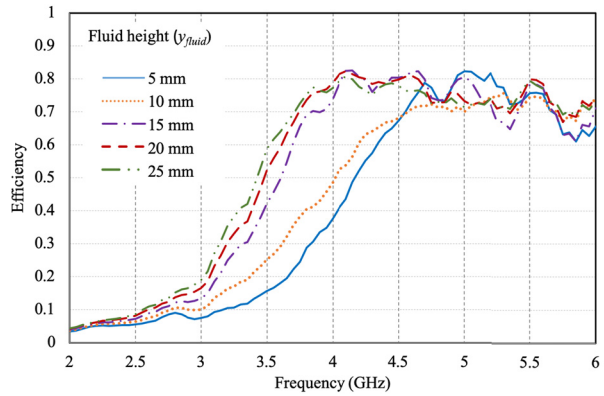

FIGURE 8. Total efficiency against frequency of the AUT at different fluid heights.

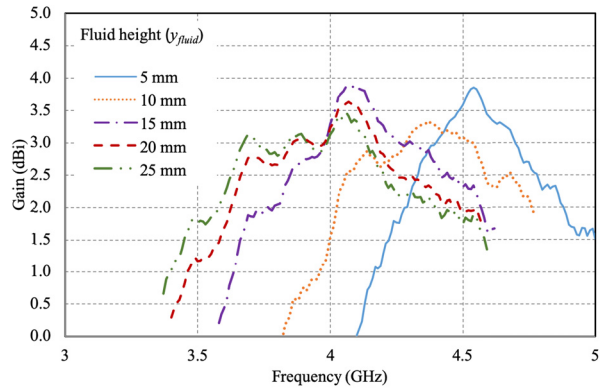

FIGURE 9. Maximum gain of the AUT at different fluid heights vs frequency.

the 3D-printed monopole antenna. The measured result also agrees reasonably with the simulated result at $y_{fluid} = 15$ mm. Fig. 8 shows the measured efficiency of the antenna over frequency for the different heights of the fluid. The maximum efficiency is about 80%.

Fig. 9 presents the gain in dBi from 3 to 5 GHz for different operating frequencies of the AUT. With a maximum gain of 3.8 dBi at the 4.5 GHz when the fluid height is 5 mm. The peak of the gain corresponds to the operating frequency bands shown in S_{11} result.

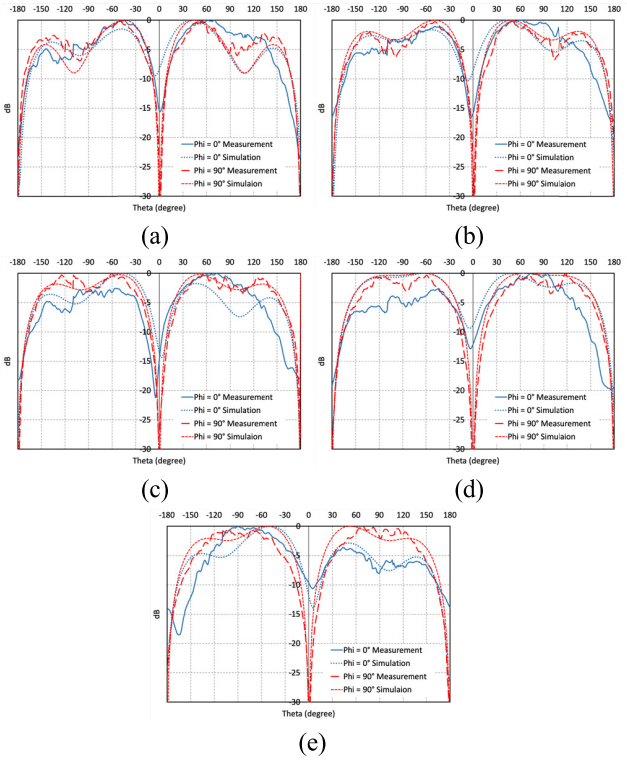

FIGURE 10. Radiation patterns of the AUT for different fluid heights at frequency point of its minimum S_{11}. (a) 5 mm at 4.55 GHz, (b) 10 mm at 4.4 GHz, (c) 15 mm at 4 GHz, (d) 20 mm at 3.7 GHz, (e) 25 mm at 3.5 GHz.

The radiation patterns of the AUT at different fluid heights are also measured to verify the performance of the antennas. Fig. 10 shows the measured radiation patterns of the AUT for different fluid heights at the frequency point of its minimum S_{11} parameter presented in Fig. 7. The measurements were performed in an anechoic chamber. Two cuts in E-plane (Phi = 0° and Phi = 90°) at the AUT's minimum S_{11} frequency points are presented. The measured radiation patterns are stable in all operating bands and are in reasonable agreement with a conventional monopole antenna and the simulated radiation patterns considering the presence of the RF cables and adaptors in the measurement.

VII. DISCUSSION

The design process of a fluidic antenna system has been demonstrated through three parts: driving the pump to produce an accurate fluid height control, sending the command to Raspberry Pi from PC to control the pump indirectly, and obtaining the S-parameters data from VNA by PC in real time, which corresponds to the three main elements in a closed-loop system: actuator, controller and feedback.

The measurement of S_{11} of the coupling-fed fluidic monopole antenna reflects the frequency agility of the proposed antenna. The resonant frequency of the fluidic monopole antenna decreases with the increasing height of fluid inside the tube. Within the 20 mm difference in the fluid height, the operating frequency of the antenna can be tuned between 3.2 GHz to 5.0 GHz, i.e. 43.9% of the

TABLE 2. Comparison with other proposed designs.

Ref.	Antenna type	Tuning range (GHz)	Gain (dBi)	Method
[16]	Microstrip monopole with water channels	4.44-5.82	0.3-2.4	Syringe
[17]	Mercury monopole	1.7–4.9	0.5-2.3	Syringe
[18]	Mercury monopole	1.29–5.17	2.6	Micropump
This work	**Ionized water Monopole**	**3.2–5.0**	**3.0–3.8**	**Closed-loop system**

impedance bandwidth, providing the opportunity to control and adjust the operating frequency for different applications with a low-loss and low-cost method. The coupling feed geometry supports a wide impedance matching at the center frequency, i.e. 4 GHz, while the impedance becomes worse as the height changes. The proposed antenna can be dynamically controlled to cover different 5G mid-bands, particularly the 3.3 – 3.8 GHz, 4.5 – 5 GHz and 3.8 – 4.2 GHz bands for mobile applications in different countries [30]. The proposed system could be suitable for multiple communications applications that require a good mixture of coverage and capacity, which is expected to form the basis of many initial 5G services.

Table 2 presents the specifications of a selection of the most recently reported monopole fluidic antenna designs for the comparisons with the proposed design in this paper. The tuning frequency of the antennas are all in the GHz range. Difference gain values are obtained in different operating bands. And the method indicates the tuning method used, either manually using a syringe, with a micro-pump or with a closed-loop system. Most designs trade off gain in order to achieve wider frequency tuning range [16], [18]. Although other designs may present wider tuning frequency range, the design we proposed presents more stable gain in its operating bands with appropriate tuning frequency range for 5G mid-bands services. Efficiency in the design presented here is about 80%, which is comparable to other proposed designs (90.4% in [16], 85% in [17]) and greater than 54% in [18].

VIII. CONCLUSION

A novel closed-loop fluidic antenna system, which is able to reconfigure itself in real time to operate at a desirable working frequency for different communication environment and applications with stable transmission of signal, has been proposed. The frequency agility of fluidic monopole antenna is achieved by automatically adjusting the height of ionized solution inside the watertight 3D-printed tube. A parametric study has also been provided for references. The proposed antenna could be useful for the applications in the recently released 5G mid-bands operations.

ACKNOWLEDGMENT

The authors would also like to thank Dr. Jie Sun and Dr. Wing Chi Mok from the State Key Laboratory of Millimeter Waves at City University of Hong Kong for their support in measuring the efficiency of the antenna.

REFERENCES

[1] J. Kiriazi, H. Ghali, H. Ragaie, and H. Haddara, "Reconfigurable dual-band dipole antenna on silicon using series MEMS switches," in *Proc. IEEE Antennas Propag. Soc. Int. Symp.*, Jun. 2003, pp. 403–406.

[2] K. M. Ho, S. Member, and G. M. Rebeiz, "Polarization diversity and frequency agility," *IEEE Trans. Antennas Propag.*, vol. 62, no. 5, pp. 2398–2406, May 2014.

[3] C. W. Jung, Y. J. Kim, Y. E. Kim, and F. De Flaviis, "Macro-micro frequency tuning antenna for reconfigurable wireless communication systems," *Electron. Lett.*, vol. 43, no. 4, pp. 201–202, Feb. 2007.

[4] M. R. Hamid, P. Gardner, P. S. Hall, and F. Ghanem, "Reconfigurable Vivaldi antenna with tunable stop bands," in *Proc. Int. Workshop Antenna Technol.(iWAT)*, Mar. 2011, pp. 54–57.

[5] X. Artiga, J. Perruisseau-Carrier, P. Pardo-Carrera, I. Llamas-Garro, and Z. Brito-Brito, "Halved Vivaldi antenna with reconfigurable band rejection," *IEEE Antennas Wireless Propag. Lett.*, vol. 10, pp. 56–58, 2011.

[6] J. Kim and Y. Rahmat-Samii, "Low-profile antennas for implantable medical devices: Optimized designs for antennas/human interactions," in *Proc. IEEE Antennas Propag. Soc. Symp.*, Jun. 2004, vol. 2, pp. 1331–1334.

[7] K.-F. Tong and J. Huang, "New proximity coupled feeding method for reconfigurable circularly polarized microstrip ring antennas," *IEEE Trans. Antennas Propag.*, vol. 56, no. 7, pp. 1860–1866, Jul. 2008.

[8] P. J. B. Clarricoats and H. Zhou, "The design and performance of a reconfigurable mesh reflector antenna," in *Proc. 7th IEEE Int. Conf. Antennas Propag.*, Apr. 1991, pp. 322–325.

[9] J.-C. Chiao, Y. Fu, I. M. Chio, M. DeLisio, and L.-Y. Lin, "MEMS reconfigurable Vee antenna," in *IEEE MTT-S Int. Microw. Symp. Dig.*, Jun. 1999, pp. 1515–1518.

[10] Y. Li, Z. Zhang, J. Zheng, Z. Feng, and M. F. Iskander, "Experimental analysis of a wideband pattern diversity antenna with compact reconfigurable CPW-to-slotline transition feed," *IEEE Trans. Antennas Propag.*, vol. 59, no. 11, pp. 4222–4228, Nov. 2011.

[11] G. Wang, T. Polley, A. Hunt, and J. Papapolymerou, "A high performance tunable RF MEMS switch using barium strontium titanate (BST) dielectrics for reconfigurable antennas and phased arrays," *IEEE Antennas Wireless Propag. Lett.*, vol. 4, pp. 217–220, 2005.

[12] (2015). *Radant MEMS*. [Online]. Available: http://www.radantmems.com/radantmems/products.html

[13] G. J. Hayes, J.-H. So, A. Qusba, M. D. Dickey, and G. Lazzi, "Flexible liquid metal alloy (EGaIn) microstrip patch antenna," *IEEE Trans. Antennas Propag.*, vol. 60, no. 5, pp. 2151–2156, May 2012.

[14] A. P. Saghati, J. Batra, J. Kameoka, and K. Entesari, "A microfluidically-tuned dual-band slot antenna," in *Proc. IEEE Antennas Propag. Soc. Int. Symp. (APSURSI)*, Jul. 2014, pp. 1244–1245.

[15] C. Murray and R. R. Franklin, "Independently tunable annular slot antenna resonant frequencies using fluids," *IEEE Antennas Wireless Propag. Lett.*, vol. 13, pp. 1449–1452, 2014.

[16] A. Singh, I. Goode, and C. E. Saavedra, "A multistate frequency reconfigurable monopole antenna using fluidic channels," *IEEE Antennas Wireless Propag. Lett.*, vol. 18, no. 5, pp. 856–860, May 2019.

[17] A. M. Morishita, C. K. Y. Kitamura, A. T. Ohta, and W. A. Shiroma, "A liquid-metal monopole array with tunable frequency, gain, and beam steering," *IEEE Antennas Wireless Propag. Lett.*, vol. 12, pp. 1388–1391, 2013.

[18] A. Dey, R. Guldiken, and G. Mumcu, "Microfluidically reconfigured wideband frequency-tunable liquid-metal monopole antenna," *IEEE Trans. Antennas Propag.*, vol. 64, no. 6, pp. 2572–2576, Jun. 2016.

[19] A. Dey and G. Mumcu, "Microfluidically controlled frequency-tunable monopole antenna for high-power applications," *IEEE Antennas Wireless Propag. Lett.*, vol. 15, pp. 226–229, 2016.

[20] C. Borda-Fortuny, K.-F. Tong, A. Al-Armaghany, and K.-K. Wong, "A low-cost fluid switch for frequency-reconfigurable Vivaldi antenna," *IEEE Antennas Wireless Propag. Lett.*, vol. 16, pp. 3151–3154, 2017.

[21] C. Hua and Z. Shen, "Shunt-excited sea-water monopole antenna of high efficiency," *IEEE Trans. Antennas Propag.*, vol. 63, no. 11, pp. 5185–5190, Sep. 2015.

[22] Y. Li and K.-M. Luk, "A water dense dielectric patch antenna," *IEEE Access*, vol. 3, pp. 274–280, 2015.

[23] L. C. Cadwallader, "Gallium safety in the laboratory," Idaho Nat. Eng. Environ. Lab., Idaho Falls, ID, USA, Tech. Rep. INEEL/CON-03-00078, 2003.

[24] F. Barbiera and J. Blanc, "Corrosion of martensitic and austenitic steels in liquid gallium," *J. Mater. Res.*, vol. 14, no. 3, pp. 737–744, Mar. 1999.
[25] R. A. Burton and R. G. Burton, "Control of surface attack by gallium alloys in electrical contacts," Burton Technol., Raleigh, NC, USA, Tech. Rep. DTIC ADA168168, 1986.
[26] FormLabs. *Form 1+*. Accessed: Nov. 24, 2018. [Online]. Available: https://support.formlabs.com/s/topic/0TO1Y000006mfMXWAY?language=en_US
[27] *CST Microwave Studio*, CST, Vélizy-Villacoublay, France, 2016.
[28] (2018). *Raspberry Pi User Manual*. [Online]. Available: https://www.raspberrypi-spy.co.uk/category/tutorials-help/
[29] *Portable Vector Network Analyzer*, Rohde & Schwarz, Munich, Germany, 2013.
[30] GSMA. (2018). *5G Spectrum GSMA Public Policy Position*. [Online]. Available: https://www.gsma.com/latinamerica/wp-content/uploads/2019/03/5G-Spectrum-Positions.pdf

CRISTINA BORDA-FORTUNY (M'14) received the B.S. degree in telecommunications engineering majoring in electronics and the M.S. degree in telecommunications engineering from La Salle BCN University, Barcelona, Spain, in 2010 and 2012, respectively, and the M.Res. degree in security science and the Ph.D. degree from University College London, London, U.K., in 2013 and 2017, respectively.

From 2015 to 2017, she was a Research Assistant with the UCL Sensors Systems and Circuits Group. From 2017 to 2018, she was a Postdoctoral Research Associate with Pompeu Fabra University. Since 2019, she has been an Associate Lecturer with the Engineering Department, La Salle BCN University. Her research interests include reconfigurable antennas, ultra-wideband antennas, fluid antennas, frequency agile antennas, microwave circuits, the IoT, and 5G applications. She received the La Salle URL Best Student Award.

LINYU CAI (S'19) was born in Jiangsu, China, in 1993. He received the B.S. degree in telecommunications (embed system design) from the Nanjing University of Posts & Telecommunications, in 2011, and the M.Sc. degree in wireless and optical communications from University College London (UCL), in 2012, where he is currently pursuing the Ph.D. degree. His current research interests include reconfigurable antenna design and the IoT.

KIN FAI TONG (M'99–SM'13) received the B.Eng. and Ph.D. degrees in electronic engineering from the City University of Hong Kong, in 1993 and 1997, respectively.

After graduation, Dr. Tong worked in the Department of Electronic Engineering, City University of Hong Kong, as a Research Fellow. Two years later, he took up the post Expert Researcher at the Photonic Information Technology Group and the Millimetre-Wave Devices Group, the National Institute of Information and Communications Technology (NiCT), Japan, where his main research focused on photonic-millimeter-wave planar antennas for high-speed wireless communications systems. In 2005, he started his academic career at the Department of Electronic and Electrical Engineering, UCL, as a Lecturer. He is currently a Reader in antennas, microwave and millimeter-wave engineering with the department. His current research interests include millimeter-wave antennas, fluid antennas, 3D printed antennas, and the sub-GHz long-range IoT networks. He served as the General Co-Chair of the 2017 International Workshop on Electromagnetics (iWEM) and a Subject Editor for *Electronics Letters* (IET).

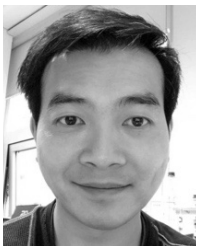

KAI-KIT WONG (M'01–SM'08–F'16) received the B.Eng., M.Phil., and Ph.D. degrees in electrical and electronic engineering from The Hong Kong University of Science and Technology, Hong Kong, in 1996, 1998, and 2001, respectively.

After graduation, he took up academic and research positions at The University of Hong Kong, Lucent Technologies, Bell-Labs, Holmdel, the Smart Antennas Research Group, Stanford University, and the University of Hull, U.K. He is currently the Chair in Wireless Communications with the Department of Electronic and Electrical Engineering, University College London, U.K. His current research interests include 5G and beyond mobile communications, including topics such as massive MIMO, full-duplex communications, millimeter-wave communications, edge caching and fog networking, physical-layer security, wireless power transfer and mobile computing, V2X communications, and, of course, cognitive radios. There are also a few other unconventional research topics that he has set his heart on, including, for example, fluid antenna communications systems and remote ECG detection.

Dr. Wong is also a Fellow the IET. He was a co-recipient of the 2013 IEEE Signal Processing Letters Best Paper Award, the 2000 IEEE VTS Japan Chapter Award at the IEEE Vehicular Technology Conference, Japan, in 2000, and a few other international best paper awards. He is also on the editorial board of several international journals. He has served as an Editor for the IEEE TRANSACTIONS ON WIRELESS COMMUNICATIONS, from 2005 to 2011, and an Associate Editor for the IEEE SIGNAL PROCESSING LETTERS, from 2009 to 2012. He was a Guest Editor of the IEEE JSAC SI on virtual MIMO, in 2013. He is also a Guest Editor for IEEE JSAC SI on physical layer security for 5G. He has been serving as a Senior Editor for the IEEE COMMUNICATIONS LETTERS, since 2012, and the IEEE WIRELESS COMMUNICATIONS LETTERS, since 2016.